

Space Qualification of Laser Diode Arrays

Elisavet Troupaki, Nasir B. Kashem, Graham R. Allan, Aleksey Vasilyev & Mark Stephen.

NASA Goddard Space Flight Center
Laser and Electro-Optics Branch, Code 554,
Greenbelt, MD 20771

Introduction

Laser instruments have great potential in enabling a new generation of remote-sensing scientific instruments. NASA's desire to employ laser instruments aboard satellites, imposes stringent reliability requirements under severe conditions. As a result of these requirements, NASA has a research program to understand, quantify and reduce the risk of failure to these instruments when deployed on satellites. Most of NASA's proposed laser missions have base-lined diode-pumped Nd:YAG lasers that generally use quasi-constant wave (QCW), 808 nm Laser Diode Arrays (LDAs). Our group has an on-going test program to measure the performance of these LDAs when operated in conditions replicating launch and orbit. In this paper, we report on the results of tests designed to measure the effect of vibration loads simulating launch into space and the radiation environment encountered on orbit. Our primary objective is to quantify the performance of the LDAs in conditions replicating those of a satellite instrument, determine their limitations and strengths which will enable better and more robust designs. To this end we have developed a systematic testing strategy to quantify the effect of environmental stresses on the optical and electrical properties of the LDA.

Experimental Procedure

We first characterize each LDA to establish a baseline for individual array performance and status (characterizing mode). The LDAs are then operated under controlled conditions for a specified number of pulses (operating mode) and remeasured to establish an initial degradation slope. To help discriminate between normal aging effects and those induced by the stress the LDAs were divided into a control group and test group. The control samples were subjected to procedures identical to the test samples except for the applied stress. Great care was taken to ensure repeatability in our test processes so any observed change may be attributed to the applied stressor rather than measurement inconsistency. The test group of LDAs were subjected to a controlled stress: either vibration or radiation and recharacterized to determine any effects of the stressor. The LDAs were again operated and remeasured to determine the degradation rate and detect longer term effects that may be attributed to the stressor.

The characterization consists of four measurements: power and spectral content, relative power per emitter and uniformity, thermography, and a microscopic facet inspection [1]. A lifetime test station is also used which allows for long term power monitoring as the device accumulates pulses. From the power measurements lasing threshold was also determined. The devices were characterized (characterization mode) under the following QCW conditions: 200 μ s current pulses of 70 A or 100 A peak at 30Hz repetition rate with a duty cycle of 0.6% while maintained at a bulk temperature of 25°C. The operating mode uses a higher pulse repetition rate of 100Hz, at a 2% duty cycle, same current and temperature, 25°C. This shortens the time to accumulate the desired 50 million pulses and is within the specified operating parameters.

We monitored a total of 12, 808nm, QCW LDAs, from different vendors, labeled (V1) and (V2). In order to minimize variations between test devices we chose LDAs from within a vendors same production run. Typical specifications of the LDAs are shown in Table 1.

Vendor	Package - Nr of bars	Output Power @ Max Current
V1	G - 2	130 W @ 70A
V2	G - 2	200 W @ 100A

Table 1. Typical optical power and current of the test LDAs.

Four LDAs formed the control group, the remaining LDAs, the test group. The test group was further sub-divided into a vibration-test group and a radiation-test group; two devices for vibration stress, two devices for γ -irradiation and the remaining four LDAs for proton irradiation. Table 2 summarizes the tests performed on each group. In the next sections we more fully describe the vibrational tests followed by the results, then the radiation tests and results.

Vibration Tests

The vibrational tests were conducted in-house at one of Goddard Space Flight Center’s vibrational-test facilities. We used two random-vibration profiles to simulate the vibration experienced by the payload during the launch phase. The first random-vibration profile was developed for the Space Transportation System (STS) and the Expendable Launch Vehicle (ELV), program and is used for random-vibration qualification testing of subsystems

Stressor	# of LDA in Test & Control	Diodes	Tests
Vibration	2 +1 control	V1	Vibration levels: 14 grms & 20 grms.
γ - irradiation	2 +1 control	V2	Radiation doses: 5krad & 200krad.
Proton irradiation	4+2 control	V1&V2	Radiation doses: 30 krad & 60krad.

Table 2. Summary of the conducted tests

and payload components of 50 lb or less [7]. The second random-vibration profile tests small, commercial components in accordance with the NASA-STD-7001, Payload Vibroacoustic Test Criteria [3]. The second profile, essentially doubles the acceleration spectral density used in Profile 1. The profiles (see Table 3) are characterized as random-vibrations applied along 3 axes to 14.1 grms and 20 grms over a frequency range of 20 to 2000Hz. Such vibrational spectra are typical of launch. The random-vibrational tests were conducted for 3 minutes along each translational axis. Our test duration of 3 minutes exceeded the two minute test requirement for a single mission [2].

Frequency (Hz)	Profile 1	Profile 2
20	.026 g ² /Hz	.052 g ² /Hz
20-50	+6 dB/octave	+6 dB/octave
50-800	.16 g ² /Hz	.32 g ² /Hz
800-2000	-6 dB/octave	-6 dB/octave
2000	.026 g ² /Hz	.052 g ² /Hz
Overall	14.1 grms	20.0 grms

Table 3. Random Vibration Profiles

Results from the Vibration Tests

The post-test characterization of the vibration test group LDAs indicates that random-vibration up to 20 grms has little or no discernable effect on the devices. The degradation slope was remeasured and determined to be the same, within experimental error, for all devices. After the extended operation and re-characterization changes were noted in the IR thermal profiles and front facet from the initial characterization. These changes are consistent with normal use and similar changes were evident on the control samples.

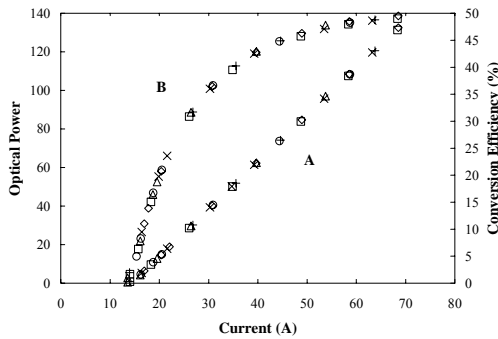


Figure 2. Optical Power (A) and Conversion Efficiency (B) as a function of laser drive current are shown for one of the devices. This graph shows that the devices are not susceptible to vibrationally induced damage up to 20 grms. The data are; \diamond - initial characterization, \triangle - after 50 million pulses, \circ - post 14 grms vibration, \square - post 14 grms & a total of 100 million pulses, \times - post 100 million pulses and post vibration to 20 grms, $+$ - post vibration to 20 grms and 150 million pulses.

- Formatted: Space Before: 1 pt, After: 1 pt
- Formatted: Space Before: 1 pt, After: 1 pt
- Formatted: Space Before: 1 pt, After: 1 pt
- Formatted: Space Before: 1 pt, After: 1 pt
- Formatted: Space Before: 1 pt, After: 1 pt
- Formatted: Space Before: 1 pt, After: 1 pt
- Formatted: Left, Space Before: 5 pt, After: 5 pt

The optical power and electrical to optical conversion efficiency as function of drive current for one device through all phases of the vibrational test is shown in Figure 2. Each curve consist of six sets of data; initial characterization, characterization after 5×10^7 shots (50 million), characterization post 14 grms vibration, characterization post 14 grms vibration and another 5×10^7 shots (100 million total), characterization post 20 grms vibration, characterization post 20 grms vibration and another 5×10^7 shots (150 million shots total). Similar graphs can be produced for all the devices tested and in each case all curves overlap. Table 4 lists the peak optical power, the center wavelength of the temporally-integrated, spectral output[1], conversion efficiency and threshold current pre- and post-vibration for the device graphed in figure 2. These devices are insensitive to random vibration along 3 axes up to 20 grms, as expected.

Time	Max Optical Power	Peak Wavelength	Threshold Current	Conversion Efficiency
	[W]	[nm]	[A]	[%]
Initial characterization	132.6	805.68	14.3	49.5
Post1st operation ($5 \cdot 10^7$ pulses)	132.4	805.70	14.4	49.6
Post vibration to 14 grms	132.3	805.70	14.3	49.3
Post 2nd operation ($5 \cdot 10^7$ pulses)	131.3	805.69	14.3	49.0
Post vibration to 20 grms	131.5	805.69	14.2	49.2
Post 3rd operation ($5 \cdot 10^7$ pulses)	132.4	805.74	14.4	49.2

Table 4. Typical values for maximum optical power, peak wavelength, threshold current and conversion efficiency before and after vibrations for a device.

Radiation Tests

The total radiation dose for space missions is predictable and vary depending on mission. The radiation flux experienced at any time depends on such parameters as transit time - for interplanetary travel, orbit type, spacecraft shielding, mission duration and solar activity. Total radiation doses are typically between 15 krad and 100 krad. For example, the radiation dose for the Ice Cloud and Elevation Satellite (ICESat) spacecraft in low, polar Earth orbit, is expected to be around 100 krad accumulated over 5 years. The MErcury Surface, Space ENvironment, GEochemistry, and Ranging (MESSENGER) spacecraft is expected to accumulate 30 krad during its 8 year exploratory mission.

To simulate the radiation expected during a typical mission we expose the LDAs to either proton or γ -radiation. Controlled exposure to high-energy protons can be used to predict the response of a device to heavy ion exposure in a wide range of Earth orbits[3]. Typical radiation dose for a space flight test are ~ 60 krad(Si) for high-energy protons and ~ 200 krad(Si) for γ -radiation. The γ -irradiation work was performed at the Johns Hopkins University Applied Physics Laboratory using a Cobalt-60 source producing γ -rays at 1.17 MeV and 1.33 MeV with nearly 100% frequency of occurrence and a dose rate equal to 744 rads (Si)/min. The samples were exposed to 5 krad(Si) and 200 krad(Si). The proton irradiation testing was performed at Indiana University Cyclotron Facility [2]. The samples were placed in the 200 MeV proton beam until they were exposed to a total dose of 30 krad or 60 krad.

We report both the threshold level and the electrical to optical power conversion efficiency pre- and post-radiation. The lasing threshold [7] is a sensitive test for radiation induced damage in LDAs. Radiation can cause internal defects within the semiconductor structure resulting in increased optical loss and decreased electrical efficiency.

Results of Proton Irradiation.

Four LDAs were irradiated with protons to the specified dose. The devices were stored until the residual activation had decayed to background levels before they were then recharacterized. The devices were essentially unaffected by the accumulated dose at the given proton flux. A slight increase in threshold-current was observed. This is consistent with defect formation within the material. Again changes were observed in the thermal profile consistent with normal use and evident on both the control and test samples. Figure 3 is a plot of the threshold-

Formatted: Space Before: 2 pt, After: 2 pt

Formatted: Space Before: 2 pt, After: 2 pt

Formatted: Space Before: 2 pt, After: 2 pt

Formatted: Space Before: 2 pt, After: 2 pt

Formatted: Space Before: 2 pt, After: 2 pt

Formatted: Space Before: 2 pt, After: 2 pt

current for each device, control group and proton-irradiated test group as a function of event. Figure 3 Left, is an expanded plot of the optical power around threshold for one device pre- and post 60 krad of proton irradiation.

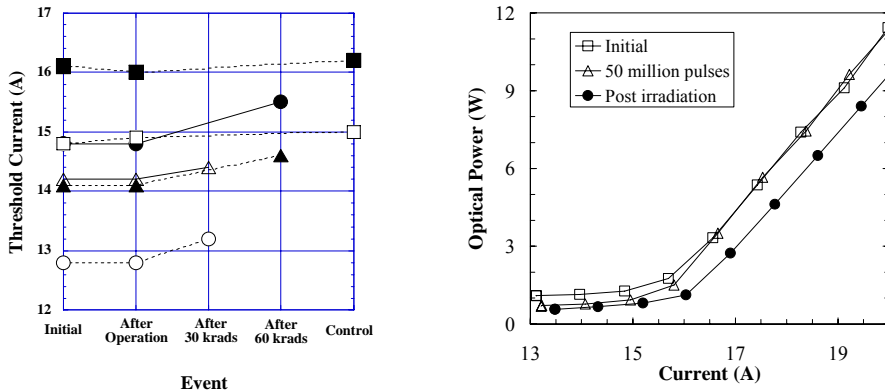


Figure 3. Threshold current for lasing pre and post-irradiation for control and test group (Left). ○ - V2 at 30 krad, ● - V2 at 60 krad, △ - V1 at 30 krad, ▲ - V1 at 60 krad, ■ - V1 control sample, □ - V2 control sample. The lines are guides for the eye. The change in threshold current is small and increases with exposure to radiation. Right is a plot of the optical power around threshold pre- and post proton irradiation.

The maximum shifts in threshold, after exposure to the highest dose, were equal to 3.5% and 4.7% of the initial threshold values for the LDAs V1 and V2 respectively. The threshold for the LDAs exposed to the lower dose also increased 1.4% (V1) and 3.1% (V2). The increase in threshold for both control samples was less than 1%. This results in a slight decrease in the conversion efficiency. These devices are currently accumulating 50 million shots and so the degradation slope, post -irradiation, was unavailable. However from observation of the optical power the degradation slope appears to be unchanged. The average optical spectra of the test LDAs also remained unchanged.

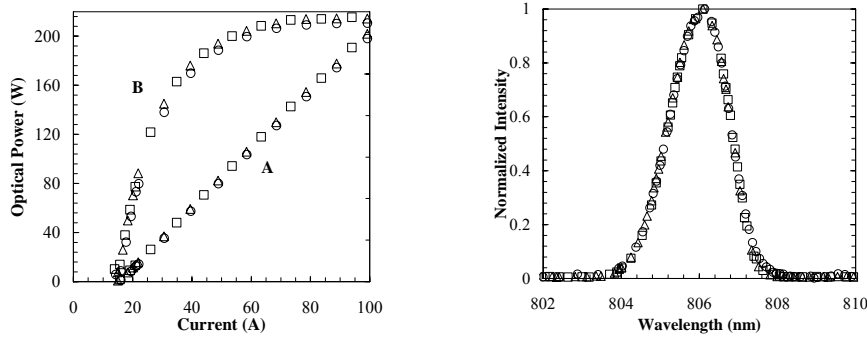


Figure 4. Left, is a plot of the optical power (A) and Conversion Efficiency (B) as a function of drive current for the LDA pre and post exposure to 60krad of proton-radiation. Right is a typical result and plots the normalized average optical spectrum pre and post exposure to 60krad of γ -radiation. △- initial characterization, □ - after operation, ○ - after irradiation (60 krad). As can be clearly seen that γ -radiation to this level and no effect on the spectra.

Results of γ -Irradiation

We γ -irradiated two LDAs with one control. This γ -irradiation was performed in two steps with an exposure rate of 744 rads (Si)/min. One device was irradiated to 5 krad(Si) and recharacterized. A second device was then added to the test group and both devices were irradiated for a second exposure of 200 krad(Si) at and recharacterized. The devices were essentially unaffected by the accumulated dose of the γ -radiation. However

changes were seen in the thermal profile consistent with normal use and evident on the control samples. The degradation slope has not been measured as we are waiting for the proton irradiated LDA "operation" to finish.

Conclusions – Future Work

Our main objective was to quantify the performance of the laser diode arrays in the conditions they are likely to encounter during a space flight. Our test protocol was designed to separate the changes due to manufacturing defects or aging from those induced by the stress parameters of vibration and radiation. Our results indicate that LDA performance is not affected by the vibration levels of 14.1 and 20 grms. Such vibration levels are higher than the vibration loads during a typical launch into space. We also observed that LDA are insensitive to γ -radiation up to 205 krad(Si). We did observe small changes in LDA performance after exposure to proton radiation. LDA threshold current was affected by proton radiation with an average increase in the threshold current of 3.2% compared to 1% for the control samples. The maximum measured increase was 4.7% for one sample. We conclude that these LDAs are robust enough to survive the vibration and radiation stresses of most space flight missions.

Future work will expand the proton irradiation test to include testing to higher doses and with different proton energies.

Acknowledgements The authors would like to acknowledge the assistance of Matt Bevan at the Johns Hopkins University Applied Physics Lab and helpful discussions with Melanie Ott in the Parts, Packaging and Assembly Technologies Office at Goddard Space Flight Center.

References

- [1] Alex Vasilyev, Graham R. Allan, John Schafer, Mark A. Stephen and Stefano Young, "Optical & Thermal Analyses of High-Power Laser Diode Arrays", *Technical Digest, Seventeenth Solid State and Diode Laser Technology Review*, p-38, 8-10 June, 2004 Albuquerque, New Mexico.
- [2] General Environmental Verification Specification (GEVS) for STS and ELV Payloads, Subsystem and Components, <http://arioch.gsfc.nasa.gov/302/gevs-se/toc.htm>
- [3] Payload Vibroacoustic Test Criteria, NASA-STD-7001, June 21, 1996
- [4] Dynamic Environmental Criteria, NASA-HDBK-7005, March 13, 2001
- [5] Petersen E.L., "The SEU Figure of Merit and Proton Upset Rate Calculations", *IEEE Trans. Nucl. Sc.*, vol. 45/6, pp. 2550-2562, 1998.
- [6] B. von Przewoski, T. Rinckel, W. Manwaring, G. Broxton, M. Chipara, T. Ellis, E.R. Hall, A. Kinser, "Beam Properties of the new Radiation Effects Research Stations at Indiana University Cyclotron Facility", *Nuclear Space Radiation Effects Conference, Data Workshop*, Atlanta, Ga, 19-23 July 2004.
- [7] Johnston A.H., "Radiation Degradation Mechanisms in Laser Diodes", *IEEE Trans. Nucl. Sc.*, Vol. 51, No 6, Dec. 2004.